



Therapeutic effect of selenium and vitamin E on arsenic induced cardiac damage in adult male albino rat: Histological, biochemical and pharmacological study

Radwa Mohammed Ahmed¹, Sarwat Lotfi Ahmed Abdel-Latif², Mostafa Yehia Abdelwahed³, Mohamed Hussein Elmahdi⁴, Ayman Mohamed Helal⁵, Heba Hussein Rohym⁶

¹Lecturer, Anatomy and Embryology Department, Faculty of Medicine, Fayoum University, Egypt

²Lecturer, Histology Department, Faculty of Medicine, Fayoum University, Egypt

³Lecturer, Physiology Department, Faculty of Medicine, Fayoum University, Egypt

⁴Lecturer, Pathology Department, Faculty of Medicine, Fayoum University, Egypt

⁵Lecturer, Pharmacology Department, Faculty of Medicine, Fayoum University, Egypt

⁶Lecturer, Forensic Medicine and Clinical Toxicology Department, Faculty of Medicine, Fayoum University, Egypt

Abstract: Introduction: Arsenic is present naturally in drinking water, soil and air. Exposure to it via drinking water is associated with cardiomyopathy and ischemic heart disease, hypertension, peripheral vascular disease. Selenium and vitamin E co-administration markedly improves the deleterious effect of arsenic in rat myocardium. Both agents are natural antioxidants used to decrease tissue inflammatory reaction exerted by free oxygen radicals. Each drug could be used alone in treatment of sodium arsenate induced myocardial damage. However, combined administration of both drugs has a more potent anti-oxidant and antiapoptotic effect compared to using each drug alone. **Aim of work:** to elucidate the therapeutic role of selenium and vitamin E on sodium arsenate induced histological and biochemical alterations on rat myocardium. Material and methods: Fifty adult male albino rats were divided into five groups, weighing 180-220 g; **Group I (Normal control):** The rats were injected intraperitoneally once daily with 0.9% saline. **Group II (Sodium arsenate administration for two weeks):** The rats were injected intraperitoneally with 7.2mg/kg/day of sodium arsenate for two weeks. **Group III (Sodium arsenate administration for six weeks):** The rats were injected intraperitoneally with 7.2mg /kg/day of sodium arsenate for six weeks. **Group IV (Sodium arsenate for two weeks then selenium +vitamin E co-administration):** The rats were injected intraperitoneally with 7.2mg/kg/day of sodium arsenate for two weeks followed by co administration with both 10 µg / kg / day selenium, and 20 mg / kg / day vitamin E for another two weeks. **Group V (Sodium arsenate for six weeks then selenium +vitamin E co-administration):** The rats were injected intraperitoneally with 7.2mg/kg/day of sodium arsenate for six weeks followed by co administration with both 10 µg / kg / day selenium, and 20 mg / kg / day vitamin E for another two weeks. The heart was excised and processed for the following studies: Light microscopic study with hematoxylin and eosin (H & E) and Masson's trichrome stains, electron microscopic examination and biochemical estimation of antioxidant enzymes. **Results:** Examination of specimens of the group treated with sodium arsenate revealed disturbed myocardial architecture, nuclear and cytoplasmic degeneration, myocardial fibrosis and marked reduction of tissue levels of antioxidant enzymes. However, selenium –vitamin E co-administration markedly ameliorated these histological and biochemical alterations. **Conclusion:** It could be concluded that selenium and vitamin E had a beneficial role in treatment of cardiomyopathy caused by sodium arsenate administration in adult male albino rats.

[Radwa Mohammed Ahmed, Sarwat Lotfi Ahmed Abdel-Latif, Mostafa Yehia Abdelwahed, Mohamed Hussein Elmahdi, Ayman Mohamed Helal, Heba Hussein Rohym. **Therapeutic effect of selenium and vitamin E on arsenic induced cardiac damage in adult male albino rat: Histological, biochemical and pharmacological study.** *Life Sci J* 2020;17(9):71-83]. ISSN: 1097-8135 (Print) / ISSN: 2372-613X (Online). <http://www.lifesciencesite.com>. 9. doi:[10.7537/marslsj170920.09](https://doi.org/10.7537/marslsj170920.09).

Keywords: Sodium arsenate, Selenium, vitamin E, Heart.

1. Introduction

Arsenic is present naturally in drinking water, soil and air. It is used as a semiconductor and in wood preservation. It causes oxidative damage in all body organs through increasing production of reactive oxygen species (ROS). In the liver it is methylated forming mono-methylated arsenic acid and di-

methylated arsenic acid. Exposure to arsenic through drinking water is correlated with cardiomyopathy, ischemic heart disease, hypertension, and peripheral vascular disease. Long-term exposure to arsenic has a major role in myocardial tissue disease pathogenesis

resulting in myocardial damage and cardiovascular complications (Tseng, 2007 and Wang et al, 2013).

Selenium is an essential trace element. Studies have highlighted its role as a potent antioxidant. Pre-treatment with selenium was proven to protect the frontal cortex and hippocampus of the brain against restraint stress-induced oxidative damage. Selenium was also shown to exert protective effects against aluminum-induced liver- and cadmium-induced testicular injuries respectively (Battin et al, 2006).

Vitamin E is a vitamin soluble in fat. It contains four tocopherols, namely α , β , δ , and γ . Furthermore does it contain four tocotrienols, namely α , β , δ , and γ . This vitamin plays a role in forming red blood cells and in preventing oxidation in the cells of the body. It is found in adequate amounts in whole grains e. g. oat and wheat, germs of wheat, green leafy vegetables, egg yolks, seeds and sardines. Vitamin E deficiency may be one of the causes of heart disease, Alzheimer's, diabetes and cancer. Of all biological membranes, both tocopherols and tocotrienols are essential constituents. They were proven to possess both antioxidant and non-antioxidant effects. (De Arriba et al, 2009; Elsy et al, 2018 and Zhao et al, 2019). The administration of vitamin E improved the histological alterations on rat myocardium induced by streptozotocin and different environmental toxins such as sodium arsenate markedly. Its effect was attributed to inhibition of oxidation, red blood cell formation, and prevention of body tissue breakdown. Vitamin E was also shown to prevent lipid peroxidation. It can lower the rate of lipid peroxidation as well as blood lipid levels in diabetic patients significantly. (Djurašević et al, 2008). This vitamin also exerted protective effects against pulmonary fibrosis that was induced by bleomycin hydrochloride in rats. Alpha-tocopherol as such proved to be effective in the prevention of nephrotoxicity induced by cisplatin. It was also shown to counteract hypercholesterolemia-induced age-related diseases as well as vascular complication in spinal cord reperfusion injury in rats. (Maliakel et al, 2008; Morsy et al, 2010 and Catalgol and Ozer, 2012)

Aim of work

Our goal was to ascertain the therapeutic role of selenium and vitamin E on the histological and biochemical alterations in the rat myocardium induced by sodium arsenate.

2. Material and methods

Chemicals

1-Sodium arsenate: Has been obtained by Sigma Chemical Co. It was available as a powder that was dissolved at a concentration of 0.4 ppm in tap water, which is equal to 0.4mg/l (Chattopadhyay, et al, 2003).

2- Selenium: Was purchased as sodium selenite from Sigma Aldrich Company (St. Louis, MO63103 USA). It was supplied as a white powder shape and diluted in 0.9 % sodium chloride (Avlan et al, 2005).

3-Vitamin E: Was purchased from Pharco, Alexandria, Egypt. It was provided as 400mg capsules.

Rats received the drugs at the following doses: Sodium arsenate:7.2mg/kg/day, sodium selenite: 10 μ g/kg/day, vitamin E: 20 mg/kg/day (Bhattacharjee and Pal, 2014)

Animals and experimental design

This study used Fifty adult male albino rats weighing 180-220 g. They were gathered from the House of Animal, Faculty of Medicine, Cairo University. Under standard laboratory and environmental conditions, the rats were lodged in separate cages with standard rat chow. The rats were split into five groups of 10 rats each:

Group I (Normal control): Rats of this group have been injected intraperitoneally once daily with 0.9% saline.

Group II (Sodium arsenate administration for two weeks): The rats of this group were injected intraperitoneally with 7.2mg of sodium arsenate /kg/day for two weeks.

Group III (Sodium arsenate administration for six weeks): The rats of this group were injected intraperitoneally with 7.2mg/kg/day of sodium arsenate for six weeks.

Group IV (Sodium arsenate for two weeks then selenium +vitamin E co-administration): The rats of this group were injected intraperitoneally with 7.2mg/kg/day of sodium arsenate for two weeks followed by co-administration orally, with both 10 μ g / kg / day selenium, and 20 mg / kg / day vitamin E for another two weeks.

Group V (Sodium arsenate for six weeks then selenium +vitamin E co-administration): The rats of this group were injected intraperitoneally with 7.2mg/kg/day of sodium arsenate for six weeks followed by co-administration orally, with both selenium at a dose of 10 μ g/kg/day and vitamin E at a dose of 20mg/kg/day for another two weeks. Rats have been handled according to the ethical standards accepted by the University of Cairo 's animal committee.

Methods

The heart of the experimental rats was excised and processed for the following studies:

1. Light microscopic study hematoxylin and eosin and Masson's trichrome stains.
2. Electron microscopic examination.

3. Antioxidant enzymes: Cardiac super oxide dismutase (SOD) and catalase enzymes.
4. Statistical analysis.

Methods of light microscopy (Calvi et al, 2012)

A- Hematoxylin and eosin stain

The muscle tissue was fixed in 4% paraformaldehyde. The histological sections in xylene were deparaffinized, rehydrated by a graded sequence of ethanol, and washed in running water. The sections were subsequently submerged for two minutes in Harris hematoxylin, washed in running water (five minutes), rinsed in distilled water (one minute), dyed in eosin aqueous solution (five minutes), and dehydrated in ascending concentrations of ethanol. The sections were then cleared in xylene (three successive changes, one minute each) and placed under the cover-slip.

B- Masson's trichrome stain

The histological sections were deparaffinized, rehydrated, washed in running water (two minutes), soaked in 5% iron alum (ten minutes) and Regaud's hematoxylin (three minutes), and rinsed in distilled water, 95% alcohol, and picric alcohol. The sections were then washed in running water again (ten minutes), quickly immersed in aqueous solution of xylydine ponceau (three minutes), distilled water and 1% of glacial acetic acid and 1% of phosphomolybdic acid (three minutes). Then they were rinsed in distilled water again, submerged for 2-5 minutes in aniline blue, dehydrated, cleaned and placed under a cover-slip.

Transmission electron microscopy (TEM) study (Esteva et al, 2008)

From each equatorial heart section, small cylinders (4 mm x 1 mm x 1 mm) of tissue were prepared. These cardiac tissue samples were set at 4 °C for 48 h by immersion in vials containing 1 mL of a mixed glutaraldehyde solution 1.25% and paraformaldehyde 1% in a phosphate buffered saline solution (PBS). Samples were washed for 45 min with PBS 0.14 M (pH = 7.4). This process has been repeated three times. Samples were subjected to a 1 % osmium tetroxide (OsO₄) post-fixation process in PBS for 1 h. They then dehydrated samples in acetone. They had been left for 10 min in various solutions with increasing concentrations of acetone. Dehydrated samples were placed in the epoxide resin blocks of Spurr. Cutting the resin blocks and acquiring semi-thin sections (500- 100 nm). In order to pick the regions of interest for processing and analysis using TEM, these sections were then noted with a light microscope at a magnification of 40×. The selected regions were cut and placed in square and eyelet grids. Uranyl acetate

and lead citrate stained them so that they could be studied with TEM (Jeol S 100, USA).

Antioxidant Enzyme Activity: (Sullivan-Gunn, and Lewandowski, 2013; Alves et al, 2020)

Cardiac SOD activity, with absorbance read at 480 nm, was measured by adrenaline auto-oxidation inhibition assays. Catalase activity was assessed at 240 nm by means of the H₂O₂ decrease rate. The outcomes were represented as U/total protein mg. With a spectrophotometer (Biomate 3S, Thermo Scientific-Waltham, MA, USA), enzyme activity readings were conducted and the findings were presented as nmol/min/total protein mg. The Bradford Assay determined the concentration of proteins.

3. Results

Histological results

Group I (Normal control):

Light microscopic examination of rat heart specimens stained with hematoxylin and eosin stain showed normal architecture of myocardium, branching and anastomosing cardiac muscle fibres with oval vesicular nuclei, acidophilic sarcoplasm, spindle shaped nuclei of fibroblast in the interstitial tissue in-between and small thin-walled blood vessels (**Figs. 1,2,3**). Sections of the normal control rat heart, stained with Masson's trichrome stain visualized a normal pattern of collagen deposition, which consists of a thin layer of collagen between myocardial fibres and around blood vessels (**Fig. 4**). Electron microscopic examination of rat heart specimens revealed euchromatic nucleus with prominent nucleoli, numerous cardiac muscle fibres with numerous mitochondria between the myofibrils, alternating dark bands and light bands with regular Z lines inside and sarcomere between 2 successive Z lines (**Figs. 5, 6**).

Group II (Sodium arsenate administration for two weeks):

Light microscopic examination of rat myocardium stained with hematoxylin and eosin stain showed thickening in the wall of blood vessel, disrupted cardiac muscle fibres, widening of interstitial spaces, karyolytic nuclei and vacuolation in the wall of blood vessel and sarcoplasm of cardiac fibres (**Fig. 7**). Sections of rat myocardium, stained with Masson's trichrome stain visualized a moderate increase in the amount of collagen deposition between myocardial fibres and around blood vessels (**Fig. 8**). Electron microscopic examination of rat myocardium revealed lost normal myocardial architecture and disrupted myocardial fibres. The mitochondria were either apparently normal or ballooned with lost cristae (**Fig. 9**).

Group III (Sodium arsenate administration for six weeks):

Light microscopic examination of rat heart specimens stained with hematoxylin and eosin stain showed markedly dilated, congested and hypertrophied blood vessel with vacuolated wall and massive mononuclear cell infiltration around them. Some blood vessels exhibited split walls. There were also widened interstitial spaces between the muscle fibres, markedly increased number of fibroblasts, extravasated blood, disrupted myocardial fibres, hyaline degeneration of cardiac tissue, sarcoplasmic vacuolation as well as karyolytic and pyknotic nuclei (Figs. 10, 11, 12). Sections of rat myocardium, stained with Masson's trichrome stain visualized marked increase in the amount of collagen deposition between myocardial fibres and around blood vessels with extensively fibrosed rat myocardium (Fig. 13, 14). Electron microscopic examination of rat heart specimens of the same group revealed lost normal myocardial architecture with disrupted myofibrils, extensive sarcoplasmic rarefaction and extremely shrunken and karyolytic nuclei. Most of mitochondria appeared ballooned with lost cristae and few of them were apparently normal (Figs. 15, 16).

Group IV (Sodium arsenate for two weeks and selenium +vitamin E co-administration):

Light microscopic examination of rat heart specimens stained with hematoxylin and eosin stain showed a relatively normal pattern of myocardial fibres and their nuclei, slightly increased amount of fibroblasts and extravasated blood. Few areas of sarcoplasmic vacuolation and few karyolytic nuclei could be seen (Fig. 17). Sections of rat myocardium, stained with Masson trichrome stain displayed apparently normal collagen deposition distribution between myocardial fibres and around blood vessels (Fig. 18). Electron microscopic examination of rat heart specimens of the same group revealed apparently normal myocardial architecture; alternating dark bands and light bands with regular Z lines and sarcomeres between 2 successive Z lines. Most mitochondria appeared normal with intact cristae but few of them were ballooned with lost cristae (Figs. 19, 20).

Group V (Sodium arsenate for six weeks and selenium +vitamin E co-administration):

Light microscopic examination of rat heart specimens stained with hematoxylin and eosin stain showed a relatively normal pattern of myocardial fibres and moderately widened interstitial spaces, increased amount of fibroblasts, some disrupted myocardial fibres and congested blood vessels (Fig. 21). Sections of rat myocardium, stained with Masson's trichrome stain displayed a moderate increase in the amount of

collagen between myocardial fibres and around blood vessels (Fig. 22). Electron microscopic examination of rat heart specimens of the same group revealed relatively normal myocardial architecture with few areas of disarrayed and disrupted myofibrils. The mitochondria were either apparently normal or ballooned with lost cristae (Fig. 23).

Statistical analysis of data:

Use the statistical computer package SPSS software version 22 (SPSS Inc, USA) to organize, tabulate, and statistically analyse the data collected. Calculation was made of the mean and standard deviation. ANOVA (Variance Analysis) was used to test the difference between groups on mean values of measured heart collagen area %, multiple comparisons between pairs of groups were made using Tukey HSD (Post-hoc range test). Significance was adopted at $p \leq 0.05$ for the interpretation of the results of the Significance Tests.

Heart collagen area % was statistically significantly higher in group II (9.19 ± 0.62), III (16.84 ± 0.98), IV (5.91 ± 0.73) and V (11.12 ± 1.74) compared to control (3.49 ± 0.64) with $p < 0.0001$, $p < 0.0001$, $p = 0.011$, and $p < 0.0001$, respectively. Also, heart collagen area % was statistically significantly higher in group III (16.84 ± 0.98) but lower in group IV (5.91 ± 0.73) compared to group II (9.19 ± 0.62) with $p < 0.0001$ and $p = 0.001$, respectively. No statistically significant difference was found among group II and group V ($p = 0.055$). On the other hand, Heart collagen area % was statistically significantly lower in group IV (5.91 ± 0.73) and V (11.12 ± 1.74) compared to group III (16.84 ± 0.98) with $p < 0.0001$ in both. Also, the difference between Group IV and Group V was statistically significant with $p < 0.0001$ (Table 1, Fig. 25).

The level of superoxide dismutase (SOD) was statistically significantly lower in group II (4.27 ± 0.44), III (1.85 ± 0.72) and V (3.90 ± 0.33) compared to control (5.99 ± 0.61) where $p < 0.0001$. No statistically significant difference among the control group and group IV with $p = 0.108$. SOD level was statistically significantly lower in group III (1.85 ± 0.72) as compared to group II (4.27 ± 0.44) with $p < 0.0001$. But no statistically significant difference existed between the group II and both groups IV and V with $p = 0.075$ and 0.763 , respectively. On the other hand, SOD was statistically significantly higher in group IV (5.16 ± 0.29) and V (3.90 ± 0.33) when compared to group III (1.85 ± 0.72) with $p < 0.0001$, respectively. Also, the difference between group IV and group V was statistically significant with $p = 0.006$ (Table 2, Fig. 27).

Catalase was statistically significantly lower in group II (460.73 ± 29.70), III (310.48 ± 49.73), IV (509.58 ± 10.06) and V (415.17 ± 11.22) compared to

control (590.88 ± 34.11) with $p < 0.0001$, $p < 0.0001$, $p = 0.004$ and $p < 0.0001$, respectively. It was also statistically significantly lower in group III (310.48 ± 49.73) compared to group II (460.73 ± 29.70) with $p < 0.0001$. No statistically significant difference among the group II and both groups IV and V where $p = 0.129$ and 0.174 , respectively. On the other hand, Catalase was statistically significantly higher in group IV (509.58 ± 10.06) and V (415.17 ± 11.22) as compared to group III (310.48 ± 49.73), $p < 0.0001$. There was as well, a statistically significant difference of $p = 0.001$ between group IV and group V (Table 3, Fig. 29).

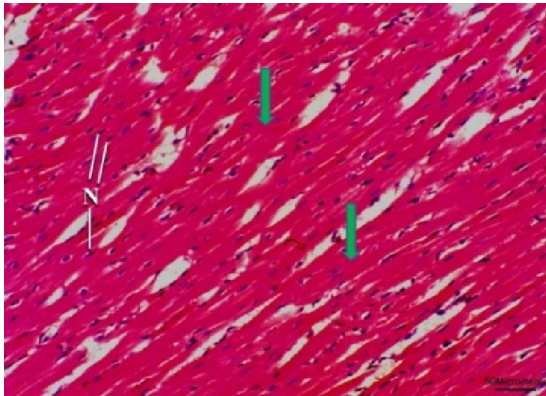


Fig. 1: A photomicrograph of a section of a rat myocardium from group I (Normal control) displaying normal myocardium architecture: branching and anastomosing cardiac muscle fibres (green arrows) with multiple central oval nuclei (N) and acidophilic sarcoplasm. (H & E x200)

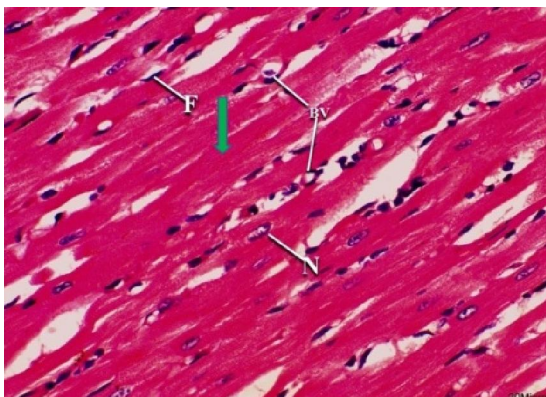


Fig. 2: A photomicrograph of a section of a rat myocardium from group I displaying normal myocardium architecture with branching and anastomosing acidophilic cardiac muscle fibres (green arrow) with oval vesicular nuclei (N). Few spindle shaped nuclei of fibroblast (F) can be observed in the interstitial tissue between the muscle fibres and around small thin walled blood vessels. (H & E x400)

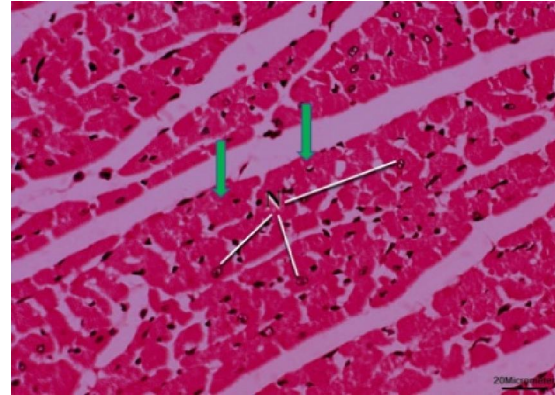


Fig. 3: A photomicrograph of a transverse section of a rat myocardium from group I displaying bundles of muscle fibres with vesicular nuclei (N) and acidophilic sarcoplasm (green arrows). (H & E x400)

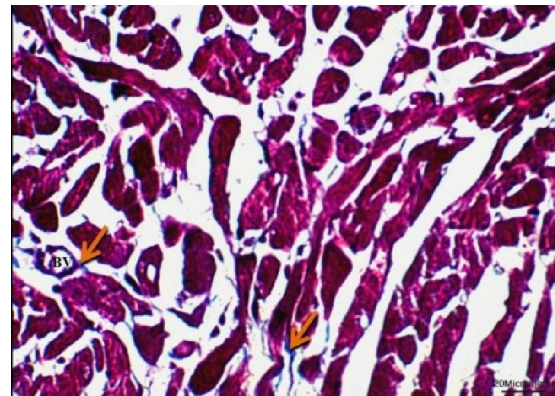


Fig. 4: A photomicrograph of a section of a rat myocardium from group I displaying a normal pattern of collagen deposition. A thin layer of collagen (arrow) is seen between myocardial fibres and around blood vessels (BV). (Masson's trichrome x400)



Fig. 5: An electron micrograph of a section of a rat myocardium from group I showing a euchromatic nucleus (N) with prominent nucleoli (n) and numerous cardiac muscle fibres with numerous mitochondria (m) between the myofibrils. (TEM x5000)

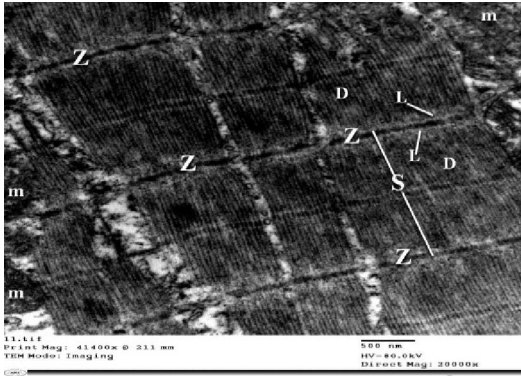


Fig. 6: An electron micrograph of a section of rat myocardium from group I showing alternating dark bands (D) and light bands (L) and regular Z lines. A sarcomere (S) lies between 2 successive Z lines. Several mitochondria are also seen (m). (TEM x20,000)

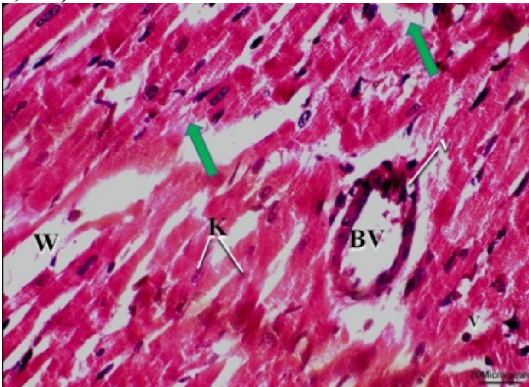


Fig. 7: A photomicrograph of a section of a rat myocardium from group II (**Sodium arsenate administration for two weeks**) showing karyolitic nuclei (K), vacuolation (v) in sarcoplasm and wall of blood vessel (BV) that exhibited thick wall, disrupted cardiac muscle fibres (green arrows), and widening of interstitial spaces (W). (H & E x400)

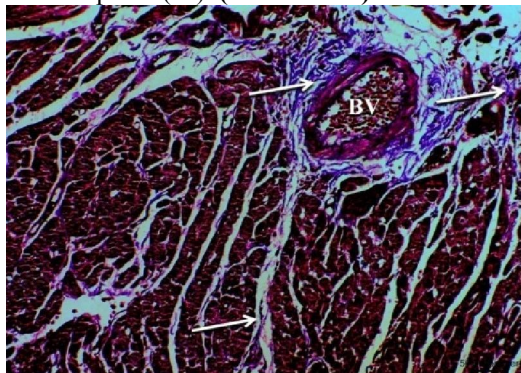


Fig. 8: A photomicrograph of a section of a rat myocardium from group II displaying moderate increase in the amount of collagen deposition (arrows) between myocardial fibres and around blood vessels (BV). (Masson's trichrome x400)

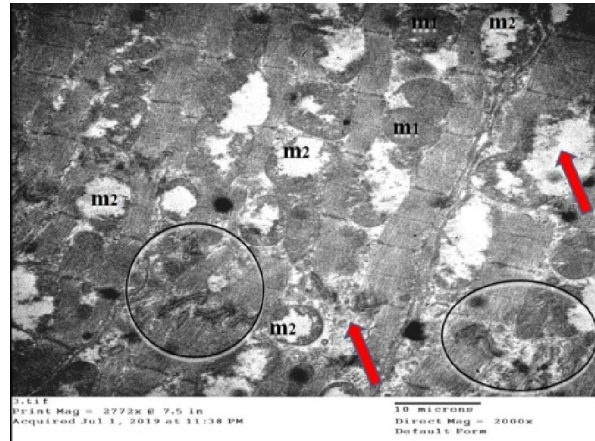


Fig. 9: An electron micrograph of a section of a rat myocardium from group II showing lost normal myocardial architecture (circle) and disrupted myocardial fibres (red arrows). The mitochondria are either apparently normal (m1) or ballooned with lost cristae (m2). (TEM x2000)

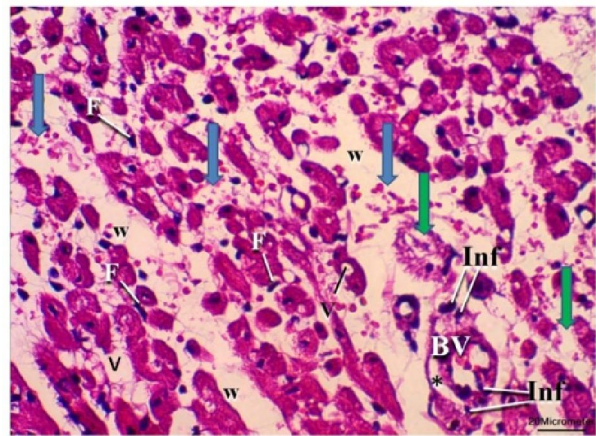


Fig. 10: A photomicrograph of a transverse section of a rat myocardium from group III (**Sodium arsenate administration for six weeks**) showing markedly widened interstitial spaces (W) and fibroblasts (F), extravasated blood (blue arrows), disrupted myocardial fibres (green arrows), mononuclear cell infiltration (Inf) around the blood vessel (BV) that exhibited a split wall (astrix). Sarcoplasmic vacuolation (v) can be visualized. (H & E x400)

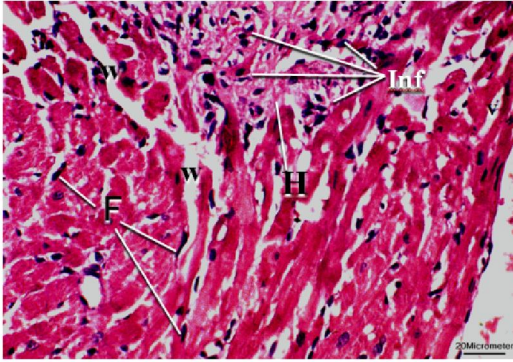


Fig. 11: A photomicrograph of a section of a rat myocardium from group (III) displaying massive, mononuclear cell infiltration (Inf), hyaline degeneration (H) of cardiac tissue, irregular arrangement of muscle fibres and widening of interstitial spaces (W) with many fibroblasts (F). (H & E x400)

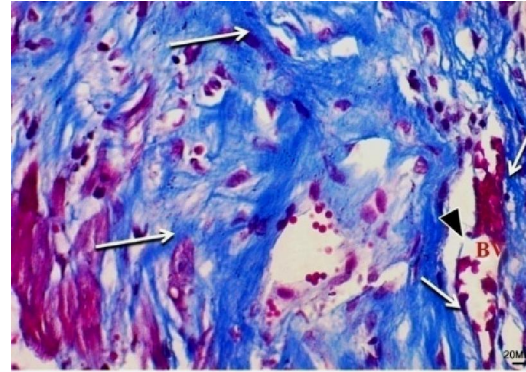


Fig.14: A photomicrograph of a section from group III displaying extensively fibrosed rat myocardium with marked increase in collagen deposition (arrows) between myocardial fibres and around blood vessels (BV). Disrupted blood vessel wall can be observed (arrowhead). (Masson's trichrome x400)

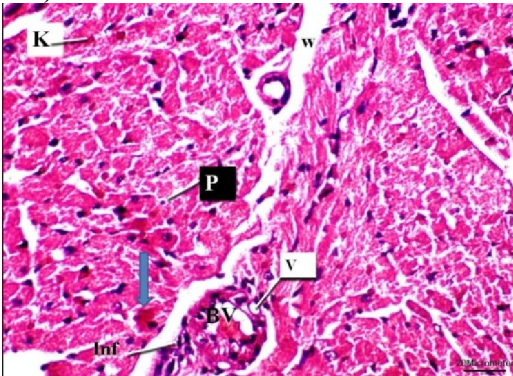


Fig. 12: A photomicrograph of a section of a rat myocardium from group (III) displaying widened interstitial spaces (W), extravasated blood (blue arrow), dilated, congested and hypertrophied blood vessel (BV) with vacuolated wall (v) and mononuclear cell infiltration (Inf) around it. Nuclear pyknosis (P) and karyolysis (K) can be seen. (H & E x400)

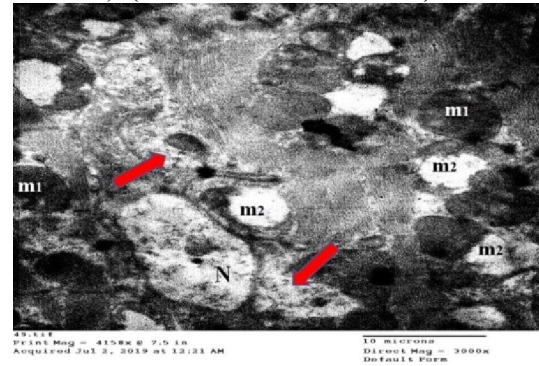


Fig.15: An electron micrograph of a section of a rat myocardium from group III displaying lost normal myocardial architecture with disrupted myofibrils (red arrow), extremely shrunken and karyolitic nucleus (N). Most of mitochondria appear ballooned with lost cristae (m2) and few of them are apparently normal (m1). (TEM x3000)

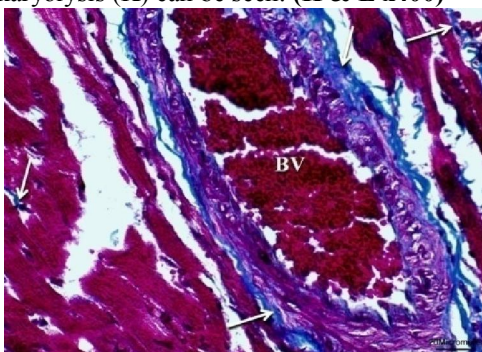


Fig.13: A photomicrograph of a section of a rat myocardium from group III displaying marked rise in collagen deposition (arrows) very prominent around congested dilated blood vessels (BV). (Masson's trichrome x400)

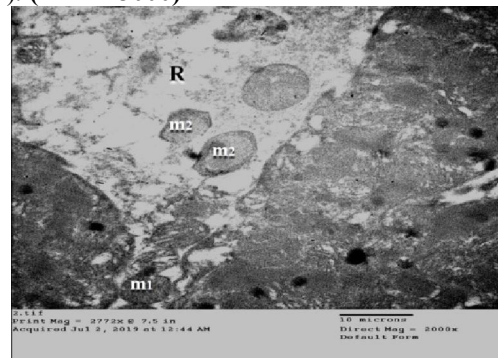


Fig.16: An electron micrograph of a section of a rat myocardium from group III showing lost normal myocardial architecture with extensive sarcoplasmic rarefaction (R). Most of the mitochondria appear ballooned with lost cristae (m2) and few of them are apparently normal (m1). (TEM x2000)

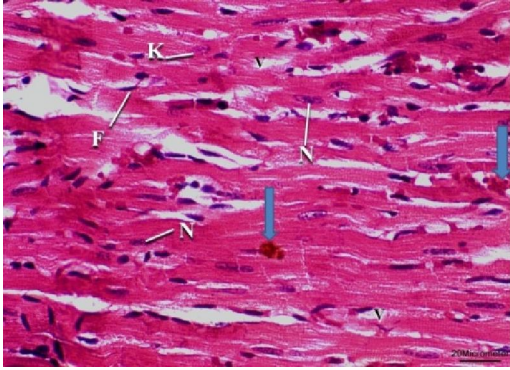


Fig. 17: A photomicrograph of a section of a rat myocardium from group IV (**Sodium arsenate for two weeks then selenium + vitamin E co-administration**) showing apparently regular branching and anastomosing pattern of myocardial fibres and their nuclei (N), some fibroblasts (F) and extravasated blood (blue arrows). Few areas of sarcoplasmic vacuolation (v) and few karyolitic nuclei (K) can be seen. (**H & E x400**)

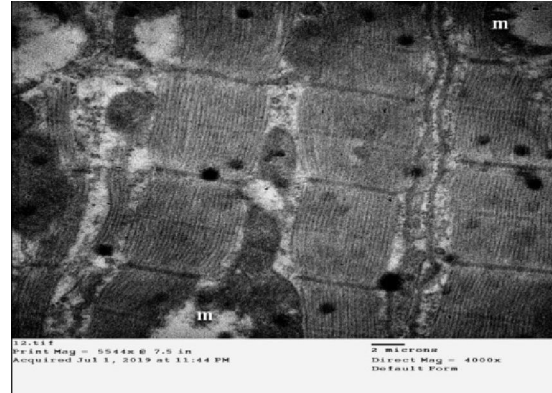


Fig.20: An electron micrograph of a section of a rat myocardium from group IV displaying relatively normal myocardial architecture. Few mitochondria (m) are ballooned with lost cristae. (**TEM x4000**)

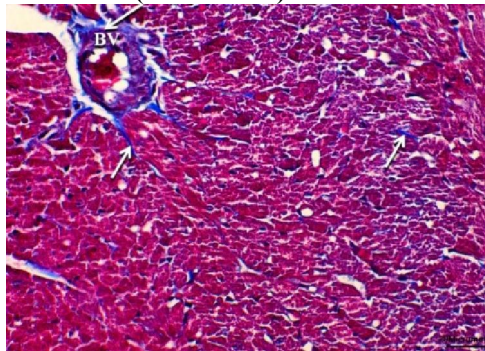


Fig.18: A photomicrograph of a section of a rat myocardium from group IV displaying apparently normal distribution of collagen (arrows) between myocardial fibres and around blood vessels (BV). (**Masson's trichrome x400**)

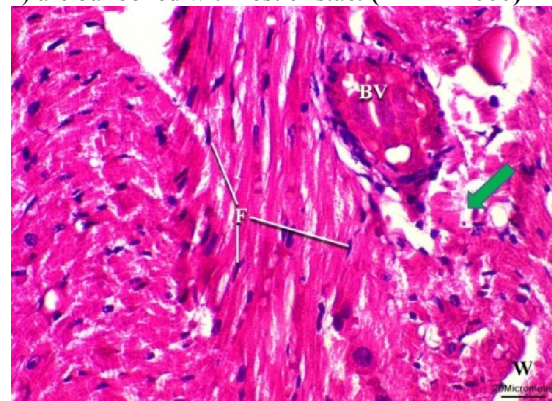


Fig. 21: A photomicrograph of a section of a rat myocardium from group V (**Sodium arsenate for six weeks then selenium +vitamin E co-administration**) showing relatively normal pattern of myocardial fibres and moderately widened interstitial spaces (W). Increased number of fibroblasts (F), disrupted myocardial fibres (green arrow), and congested blood vessel (BV) can be observed. (**H & E x400**)

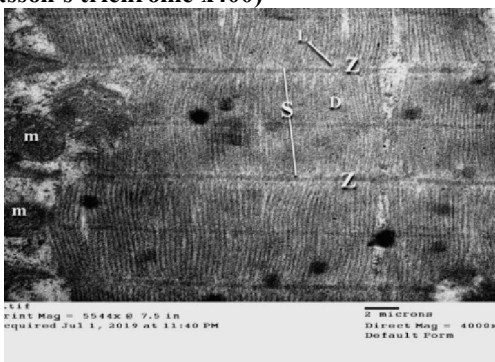


Fig.19: An electron micrograph of a section of a rat myocardium from group IV displaying seemingly normal myocardial architecture: alternating dark bands (D) and light bands (L) with regular Z lines and sarcomere (S) between 2 successive Z lines. The mitochondria are apparently normal with intact cristae (m). (**TEM x4000**)

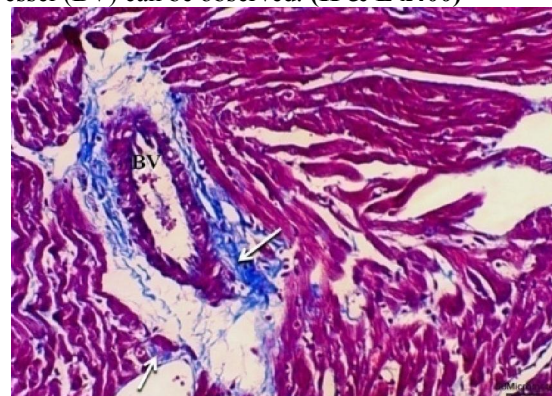


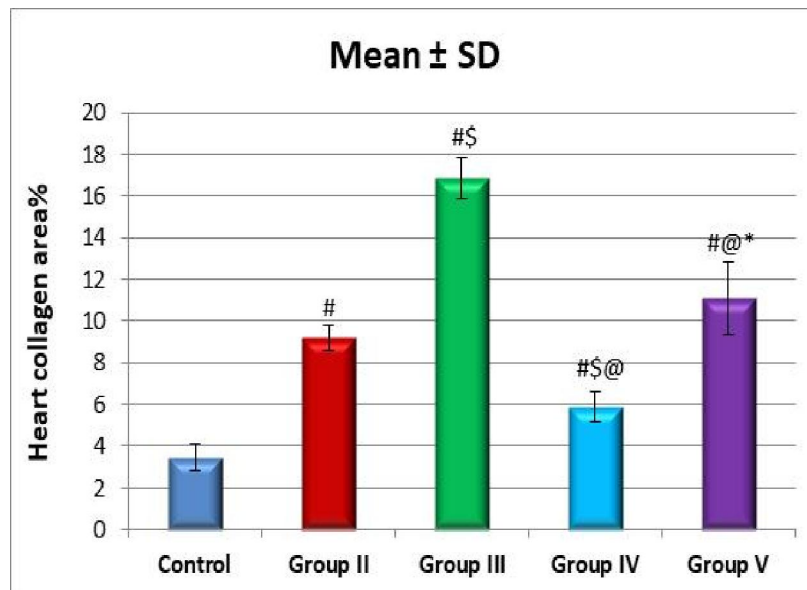
Fig.22: A photomicrograph of a section of a rat myocardium from group V displaying moderate rise in collagen (arrows) between myocardial fibres and around blood vessels (BV). (**Masson's trichrome x400**)



Fig.23: An electron micrograph of a section of a rat myocardium from group IV displaying relatively normal myocardial architecture with few areas of disarrayed (circle) and disrupted (red arrow) myofibrils. The mitochondria are either apparently normal (m1) or ballooned with lost cristae (m2). (TEM x2000)

Table 1: demonstrates area percent of collagen fibresin rat myocardium obtained from different groups of the examined animals.

	Group I (Control)		Group II		Group III		Group IV		Group V	
	Mean	SD	Mean	SD	Mean	SD	Mean	SD	Mean	SD
Collagen heart area %	3.49	0.64	9.19	0.62	16.84	0.98	5.91	0.73	11.12	1.74
P-values										
G I vs. G II	<0.0001 (S)									
G I vs. G III	<0.0001 (S)									
G I vs. G IV	0.011 (S)									
G I vs. G V	<0.0001 (S)									
G II vs. G III			<0.0001 (S)							
G II vs. G IV			0.001 (S)							
G II vs. G V			0.055 (NS)							
G III vs. G IV					<0.0001 (S)					
G III vs. G V					<0.0001 (S)					
G IV vs. G V							<0.0001 (S)			

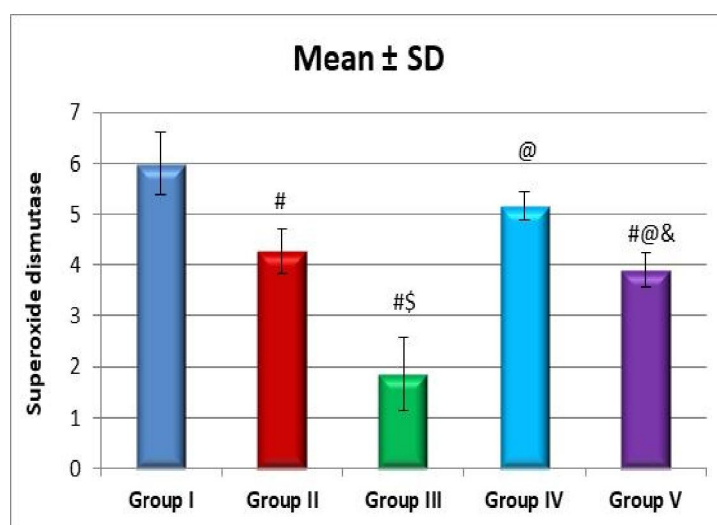


significant difference from control, \$ significant difference from group II, @ significant difference from group III, * significant difference from group IV

Fig.25: Histogram illustrating mean distribution of the connective tissue (area %) in rat myocardium obtained from different groups of the examined animals.

Table 2: demonstrates mean values of cardiac **superoxide dismutase (SOD)** levels among different study groups.

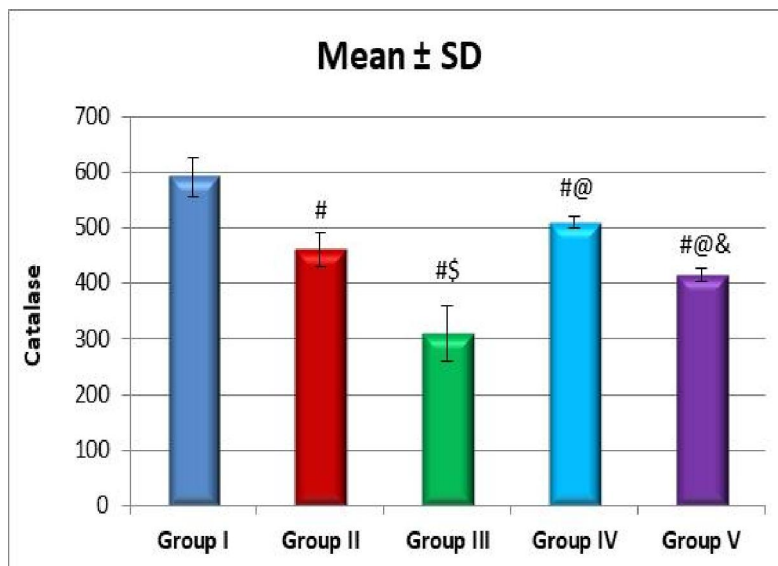
	Group I (Control)		Group II		Group III		Group IV		Group V	
	Mean	SD	Mean	SD	Mean	SD	Mean	SD	Mean	SD
SOD	5.99	0.61	4.27	0.44	1.85	0.72	5.16	0.29	3.90	0.33
P-values										
G I vs. G II	<0.0001 (S)									
G I vs. G III	<0.0001 (S)									
G I vs. G IV	0.108 (NS)									
G I vs. G V	<0.0001 (S)									
G II vs. G III	<0.0001 (S)									
G II vs. G IV	0.075 (NS)									
G II vs. G V	0.763 (NS)									
G III vs. G IV	<0.0001 (S)									
G III vs. G V	<0.0001 (S)									
G IV vs. G V	0.006 (S)									



significant difference from control, \$ significant difference from group II, @ significant difference from group III & significant difference from group IV

Fig.27: Histogram illustrating mean values of cardiac **superoxide dismutase (SOD)** obtained from the different groups of the examined animals.**Table 3:** demonstrating mean values of cardiac **Catalase** levels among different study groups.

	Group I (Control)		Group II		Group III		Group IV		Group V	
	Mean	SD	Mean	SD	Mean	SD	Mean	SD	Mean	SD
Catalase	590.88	34.11	460.73	29.70	310.48	49.73	509.58	10.06	415.17	11.22
P-values										
G I vs. G II	<0.0001 (S)									
G I vs. G III	<0.0001 (S)									
G I vs. G IV	0.004 (S)									
G I vs. G V	<0.0001 (S)									
G II vs. G III	<0.0001 (S)									
G II vs. G IV	0.129 (NS)									
G II vs. G V	0.174 (NS)									
G III vs. G IV	<0.0001 (S)									
G III vs. G V	<0.0001 (S)									
G IV vs. G V	0.001 (S)									



significant difference from control, \$ significant difference from group II, @ significant difference from group III & significant difference from group IV

Fig.29: Histogram illustrating mean values of cardiac Catalase obtained from the different groups of the examined animals.

4. Discussion

In the current study, administration of sodium arsenate resulted in marked histological alterations in the rat myocardium in the form of disturbed normal myocardial architecture, disrupted myocardial fibers, nuclear pyknosis, karyolysis, myocardial fibrosis, mononuclear cell infiltration and degenerated mitochondria. Co administration of selenium and vitamin E markedly ameliorated these alterations. Similar findings were observed by **Das et al, 2010** and **Bhattacharjee and Pal, 2014** who stated that arsenic increases production of oxidative stress which leads to myocardial damage. They added that co-administration of selenium and vitamin E is more potent than treatment with selenium or vitamin E alone when it comes to decreasing arsenate induced cardiac damage. **Li et al, 2010, Viezeliene et al, 2011, Watson et al, 2012 reported that** ROS production, the possible mechanisms of arsenic-induced cardiac damage may be DNA damage and apoptosis in the myocardial fibres. They assumed that myocardial fibrosis could be due to an increase in matrix metalloproteinases that induce tissue fibrosis. Their release is stimulated by ROS and tissue damage. **Santra et al, 2000 and Gora, et al 2014 stated that exposure to sodium arsenite results in change in myocardial and hepatic tissue architecture; haemorrhage in the myocardium as well as disruption and fibrosis of muscle fibres. Shi et al, 2004; Manna et al, 2008; Das et al, 2010; Singh and Ahluwalia,**

2012 stated that the enzyme activity of NADPH oxidase in cardiac tissue increased substantially due to arsenic toxicity and that the combined administration of vitamin E and selenium returned the enzyme activity to a higher efficacy than either of its individual supplements. Myocardial tissues are exposed to free radical damage due to decreased activities of antioxidant enzymes such as superoxide dismutase (SOD). This enzyme catalyses the dismutation of superoxide anions and prevents the subsequent formation of hydroxyl radicals.

The causative factor of the arsenic-induced SOD inhibition and catalase activities may be overproduction of superoxide anions. Decreased catalase activity indicated that exposure to arsenic results in impaired ability to detoxify H₂O₂ via catalase and hence accumulation of H₂O₂. Treatment with selenium and vitamin E prevented the reduction of antioxidant power caused by arsenic and shielded the cell from oxidative harm. They added that NADPH oxidase plays a central role in generating cardiovascular injury by ROS. Increased NADPH in arsenic-treated animals may lead to atherosclerosis and increased cholesterol. **Bau et al, 2001; Miller, et al, 2002 and Borutaite and Brown, 2003** stated that arsenic compounds may trigger apoptosis as DNA strands break due to increasing cellular nitric oxide (NO) and superoxide levels leading to inhibition of DNA repair. An enzyme that is supersensitive to arsenic is pyruvate dehydrogenase (PDH). PDH

inhibition prevents aerobic glucose oxidation and prevents the oxidative phosphorylation of ADP leading to degradation of DNA and death of cells.

Conclusion:

It could be concluded that selenium and vitamin E had a beneficial role in the treatment of cardiomyopathy induced by sodium arsenate administration in adult male albino rat.

References:

- Alves, Pereira, L. M.; Monteiro, I. C. G.; Dos-Santos, L. H. P.; Ferraz, M.; Loureiro, A. C. C.; Lima, C. C.; Leal-Cardoso, J. H.; Carvalho, D. P.; Fortunato, R. S. and Ceccatto, V. M. (2020): Strenuous Acute Exercise Induces Slow and Fast Twitch-Dependent NADPH Oxidase Expression in Rat Skeletal Muscle. *Antioxidants*, 9:57.
- Avlan, D.; Erdougan, K.; Cimen, B.; Dusmez, D.; Cinel, I. and Aksoyek, S. (2005): The protective effect of selenium on ipsilateral and contralateral testes in testicular reperfusion injury. *Pediatr. Surg. Int.*, 21:274-278.
- Bau, D. T.; Gurr, J. R. and Jan, K. Y. (2001): Nitric oxide is involved in arsenite inhibition of pyrimidine dimmer excision. *Carcinogenesis*, 22: 709–716.
- Bhattacharjee, S. and Pal, S. (2014): Additive protective effects of selenium and vitamin E against arsenic induced lipidemic and cardiotoxic effects in mice. *Int. J. Pharm. Pharm. Sci.*, 6 (5): 406-413.
- Borutaite, V. and Brown, G. C. (2003): Nitric oxide induces apoptosis via hydrogen peroxide, but necrosis via energy and thiol depletion. *Free Radic. Biol. Med.*, 35: 1457–1468.
- Calvi, E. N. V.; Nahas, F. X.; Barbosa, M. V.; Calil, J. A.; Ihara, S. S. M.; Silva, M. S.; De Franco, M. F. and Ferreira, L. M. (2012): An experimental model for the study of collagen fibers in skeletal muscle. *Acta Cirúrgica Brasileira*, 27 (10): 681- 686.
- Catalgol, B. and Ozer, N. K. (2012): Protective effects of vitamin E against hypercholesterolemia-induced age-related diseases. *Genes Nutr.* 7: 91-98.
- Chattopadhyay, S.; Pal, S.; Ghosh, D. and Debnath, J. (2003): Effect of dietary co-administration of sodium selenite on sodium arsenate- induced ovarian and uterine disorders in mature albino rat. *Toxicol. Sci.*, 75: 412-422.
- Das, A. K.; Sahu, R.; Dua, T. K.; Bag, S.; Gangopadhyay, M.; Sinha, M. K. and Dewanjee, S. (2010): Arsenic-induced myocardial injury: protective role of *Corchorus solitorius* leaves. *Food Chem. Toxicol.*, 48:1210-1217.
- De Arriba, G.; De Hornedo, J. P.; Rubio, S. R.; Fernandez, M. C.; Martinez, S. B.; Camarero, M. M. and Cid, T. P. (2009): Vitamin E protects against the mitochondrial damage caused by cyclosporin A in LLC-PK1 cells. *Toxicol. Appl. Pharmacol.*, 239: 241–250.
- Djurašević, S. F.; Djordjevic, J.; Drenca, T.; Jasnić, N. and Cvijić, G. (2008): Influence of vitamin C supplementation on the oxidative status of rat liver. *Arch Biol. Sci. Belgrade*, 60: 169-173.
- Elsy, B.; Khan, A, A, and Maheshwari, V. (2018): Co-Administered Vitamin E Isoforms d- α -tocopherol and d- δ -tocotrienol Rich Fraction Promote Regeneration of Skeletal Muscle in Diabetics. *International Journal of Nutrition and Food Sciences*, 7(2): 47-55. ckwel Publishing Ltd.
- Esteva, S.; Panisello, P.; Casas, M.; Torrella, J. R.; Pagés, T. and Viscor, G. (2008): Morphofunctional responses to anaemia in rat skeletal muscle. *Journal of Anatomy*, 212: 836-844.
- Gora, R. H.; Baxla, S. L.; Kerketta, P.; Patnaik, S. and Roy, B. K (2014): Hepatoprotective activity of *Tephrosia purpurea* against arsenic induced toxicity in rats. *Indian J. Pharmacol.*, 46: 197-200.
- Li, J. L.; Gao, R.; Li, S.; Wang, J. T.; Tang, Z. X. and Xu, S. W. (2010): Testicular toxicity induced by dietary cadmium in cocks and ameliorative effect by selenium. *Biometals*, 23: 695-705.
- Maliakel, D. M.; Kagiya, T. V. and Nair, C. K. (2008): Prevention of cisplatin induced nephrotoxicity by glucosides of ascorbic acid and alpha-tocopherol. *Exp. Toxicol. Pathol.*, 60: 521-527.
- Manna, P.; Sinha, M. and Sil, P. C. (2008): Arsenic-induced oxidative myocardial injury: protective role of arjunolic acid. *Arch Toxicol.*, 82: 137-149.
- Miller, W. H.; Schipper, H. M.; Lee, J. S.; Singer, J. and Waxman, S. (2002): Mechanisms of action of arsenic trioxide. *Cancer Res.*, 62: 3893–3903.
- Morsy, M. D.; Mostafa, O. A. and Hassan, W. N. (2010): A potential protective effect of alpha-tocopherol on vascular complication in spinal cord reperfusion injury in rats. *J. Biomed. Sci.*, 55: 1-9.
- Santra, A.; Maiti, A.; Das, S.; Lahiri, S. and Charkaborty, S. K. (2000): Hepatic damage caused by chronic arsenic toxicity in experimental animals. *Toxicol. Clin. Toxicol.* 38: 395-405.

21. Singh, K. and Ahluwalia, P. (2012): Effect of monosodium glutamate on lipidperoxidation and certain antioxidant enzymes in cardiac tissue of alcoholic adult male mice. *J. Cardiovasc. Dis. Res.*, 3: 12-18.
22. Shi, H.; Shi, X. and Liu, K. (2004): Oxidative mechanism of arsenic toxicity and carcinogenesis. *Mol Cell Biochem.*, 255: 67-78.
23. Sullivan-Gunn, M. J. and Lewandowski, P. A. (2013): Elevated hydrogen peroxide and decreased catalase and glutathione peroxidase protection are associated with aging sarcopenia. *BMC Geriatrics*, 13:104.
24. Tseng, C. H. (2007): Arsenic methylation, urinary arsenic metabolites and human diseases: Current perspective. *J. Environ. Sci. Health C., Environ. Carcinog. Ecotoxicol. Rev.*, 25: 1-22.
25. Viezeleiene, D.; Jansen, E.; Rodovicius, H.; Kasauskas, A. and Ivanov, L. (2011): Protective effect of selenium on aluminium-induced oxidative stress in mouse liver in vivo. *Environ. Toxicol. Pharmacol.* 31: 302-306.
26. Wang, H.; Xi, S.; Liu, Z.; Yang, Y.; Zheng, Q.; Wang, F.; Xu, Y.; Wang, Y.; Zheng, Y. and Sun, G. (2013): Arsenic methylation metabolism and liver injury of acute promyelocytic leukemia patients undergoing arsenic-trioxide treatment. *Environ, Toxicol*, 28: 267-275.
27. Watson, M.; Leer, V. L.; Vanderlelie, J. J. and Perkins, A. V. (2012): Selenium supplementation protects trophoblast cells from oxidative stress. *Placenta*, 33: 1012-1019.
28. Zhao, Y.; Zhang, W.; Jia, Q.; Feng, Z.; Guo, J.; Han, X.; Liu, Y.; Shang, H.; Wang, Y. and Liu, W. J. (2019): High dose of vitamin E attenuates diabetic nephropathy via alleviation of autophagic stress. *Frontiers in physiology*, 9: 1-13.

9/20/2020